IJECBE

IJECBE (2025), **3**, **3**, 544–566
Received (16 June 2025) / Revised (23 June 2025)
Accepted (24 June 2025) / Published (30 September 2025)
https://doi.org/10.62146/ijecbe.v3i3.150
https://ijecbe.ui.ac.id
ISSN 3026-5258

International Journal of Electrical, Computer and Biomedical Engineering

RESEARCH ARTICLE

Reliability Improvement of Defense Scheme Implementation Using Adaptive Load Shedding Based On System Strength Index

Dwitiya Bagus Widyantara, Iwa Garniwa*, and Fauzan Hanif Jufri

Department of Electrical Engineering, Faculty of Engineering, Universitas Indonesia, Depok, Indonesia
*Corresponding author. Email: iwa@eng.ui.ac.id

Abstract

One of the defense schemes in power systems is Under Frequency Load Shedding (UFLS), designed to mitigate cascading blackouts caused by frequency disturbances. UFLS operates based on predetermined frequency thresholds and time delays, which inherently characterizes it as a static protection mechanism and may cause unnecessary excessive or insufficient load shedding. Therefore, an Adaptive Load Shedding (ALS) approach started to gain popularity, which enables load shedding based on real-time conditions, particularly during generator outages. In this research, a comparative analysis is conducted between the conventional UFLS method and a newly developed ALS scheme that integrates the System Strength Index (SSI) to improve the system's reliability, as evaluated by Energy Not Served (ENS). The proposed ALS algorithm processes real-time feeder load data, ranks the feeders by load magnitude in descending order, and optimizes the load shedding setpoints by incorporating the SSI. The proposed method is simulated in the Flores power system model using actual historical data for two load conditions: the highest and the lowest. The results show that the proposed method outperforms the conventional UFLS by 7.31% in terms of improved ENS.

Keywords: Defense Scheme, Under Frequency Load Shedding (UFLS), Adaptive Load Shedding (ALS), System Strength Index (SSI)

1. Introduction

Frequency stability is crucial for maintaining the reliability of electric power systems. System frequency remains stable when there is a balance between power supply and demand. An imbalance between the two can lead to frequency instability, typically caused by the sudden loss of generation or disruption of the power supply from the interconnected grid [1]. Moreover, the increasing energy demand and the integration of weather-dependent renewable energy sources further contribute to the challenges of maintaining frequency stability in power systems [2]. The defense scheme of a power system refers to a series of strategies and protective measures designed to prevent or minimize the occurrence of widespread system failure caused by severe disturbances, power imbalances, or frequency instability. One of the defense schemes in electric power systems is protection against under-frequency events. This protection is typically implemented through Under Frequency Load Shedding (UFLS). The decrease of inertia in power systems due to the increasing penetration of Renewable Energy Sources (RES) affects the frequency stability of the power grid [3] [4]. The imbalance between generated power and consumed load in power systems, particularly in islanded microgrids, often leads to frequency instability. During sudden power deficits, such as disconnection from the main grid or significant drops in generation, conventional frequency control mechanisms, like Automatic Generation Control (AGC), are unable to prevent rapid frequency decline effectively [5].

The UFLS scheme consists of two types: manual and automatic. The manual UFLS scheme involves the load-shedding process, which is carried out through load-disconnection commands issued by dispatchers to the substations. [6] The automatic UFLS scheme is classified into two categories: the first is the conventional UFLS, which operates based on predetermined frequency thresholds and time delays, making it inherently static; the second is the advanced UFLS, which operates based on computational methods or even artificial intelligence. In terms of implementation speed, conventional UFLS is easier to deploy within the system. In contrast, advanced UFLS requires consideration of factors such as load transfer, available generation sources, and other system dynamics.

With the increasing penetration of renewable energy sources, the limitations of conventional defense schemes have become more apparent. Research [7] highlights that the integration of inverter-based generation, such as photovoltaic (PV) systems, leads to a decrease in system inertia, resulting in faster frequency dynamics that cannot be adequately addressed by conventional Under-Frequency Load Shedding (UFLS) schemes. Moreover, the stabilization process under conventional defense schemes tends to be delayed because load shedding is performed step-by-step, requiring a longer duration to achieve system stability following a disturbance. Such delays may significantly increase the risk of system collapse if the system's response is not sufficiently prompt [6]-[7]. In complex disturbance scenarios, it is not only the amount of load that must be shed but also the location of the load shedding that plays a critical role in maintaining system stability [8]. Conventional load-shedding methods are often inefficient because they do not account for the specific conditions of each load bus. Typically, all load buses share the power imbalance indiscriminately, which can be impractical in complex power systems [9]. Static load shedding schemes typically disconnect a fixed amount of load at each shedding stage. This approach can lead to either excessive or inadequate load shedding, making it suboptimal for maintaining system stability [10]. The phenomenon of low inertia makes the power system more vulnerable to extreme frequency fluctuations, thereby requiring protection systems to be more adaptive, responsive, and efficient [11].

In the Muarakarang subsystem, the defense scheme's failure was caused by feeder and transformer load conditions that deviated from predictions, along with suboptimal settings of the Under-Frequency Load Shedding (UFLS) system [12]. These inconsistencies resulted in existing defense schemes, such as Overload Shedding (OLS) and UFLS, being unable to effectively maintain the balance between load and generation during disturbances in the 500 kV Java-Bali transmission system. The inability of these schemes to adapt to system dynamics heightened the risk of tripping critical equipment, particularly the Interconnecting Bus Transformer (IBT), ultimately leading to a loss of power supply and resulting in a blackout within the Muarakarang subsystem. The issue of dynamic power transfer in the Java-Bali system was also observed in the study [13]. Due to the highly dynamic nature of the transfer characteristics, the existing Overload Shedding (OLS) system must be capable of dynamically adjusting the loads to be disconnected in response to variations in Java-Bali power transfer.

In response to the issue, given the uncertainties and high variability of loads and renewable energy sources, there is a need for UFLS techniques capable of automatically adjusting in real time [14]. Adaptive Defense Schemes have been introduced to address the challenges of modern electric power systems, such as the implementation in the Muara Karang subsystem, which effectively mitigated critical issues related to is-landing operation failures under certain disturbance conditions that led to power outages in the area [12]. In the study [13], the Adaptive Defense Scheme, when combined with a MySQL (Structured Query Language) database, enables comprehensive testing under conditions that closely resemble the actual operating environment of the Bali subsystem. This approach enables the system to accurately identify shedding targets with a precision rate of up to 100% while minimizing trip quota deviations to an average of only 1.03% [15]. By integrating the kinetic energy indicator (KEMI) and MLSA, this scheme can adjust load-shedding actions promptly in response to real-time system conditions. This research confirms that the approach based on the kinetic energy model and the kinetic energy indicator (KEMI) can enhance the effectiveness of the AUFLS scheme in maintaining the stability of power systems, particularly as they become increasingly complex and diverse in terms of energy sources. In the study [16], an accurate estimation of the Under Frequency Load Shedding (UFLS) amount was performed on a small power system characterized by complex frequency dynamics, achieving a Mean Absolute Error (MAE) of 0.179 MW on the test data. Particle Swarm Optimization (PSO) enhances under-frequency load shedding by accurately forecasting the system's minimum frequency after a disturbance using frequency samples without relying on precise knowledge of system parameters or direct measurement of frequency derivatives, which are prone to error in traditional methods [17].

In the study [18], an approach based on Empirical Mode Decomposition (EMD) and synchrophasor measurement was proposed to enhance the sensitivity of the UFLS scheme to rapid and complex frequency variations. This technique enables load shedding to be executed more selectively and in a more timely manner. This approach was further enhanced using adaptive methods based on Artificial Neural Networks

(ANN), which can determine the required amount of load to be shed simultaneously and more rapidly than conventional methods, with algorithm computation times of less than 10 seconds [19]. Furthermore, the spinning reserve in power system operations significantly influences the load-shedding quota, which is directly related to overall system stability [12]. In implementing Adaptive Under Frequency Load Shedding (AUFLS), it is essential to consider the emerging characteristics of modern power systems, which are increasingly dominated by renewable energy sources and energy storage systems. These components significantly affect system frequency dynamics [20]. This study employs a simple and effective adaptive load-shedding method that is feasible for actual implementation in power systems. Through this study, an evaluation of system performance in responding to disturbances is conducted by applying two types of protection schemes Under Frequency Load Shedding (UFLS) and Adaptive Load Shedding (ALS). The analysis aims to assess the effectiveness of each scheme in maintaining frequency stability and overall system reliability. Furthermore, this study quantifies the Energy Not Served (ENS) produced by each scheme as a quantitative indicator of protection performance, while also evaluating the extent to which implementing ALS based on the System Strength Index (SSI) can enhance the reliability of the Flores power system compared to the conventional UFLS scheme.

2. Flores System and The Existing Defense Scheme

One of the developing power systems in Indonesia is the Flores Power System. This system is managed by PLN UIW NTT, with the highest peak load (PL) recorded in 2023 at 90.01 MW and a total available capacity (TAC) of 105.50 MW. The Flores System consists of five subsystems: Labuan Bajo, Ruteng–Ulumbu–Borong, Bajawa–Aesesa, Ropa–Ende, and Maumere–Wairita. These subsystems are interconnected through 150 kV and 70 kV high voltage overhead transmission lines. Flores Island is one of the tourist destinations, including Labuan Bajo, which has been designated as one of Indonesia's super-priority tourism development zones. Labuan Bajo has hosted several international events, such as the 42nd ASEAN Summit, G20 side events, and the 2023 Asia–Australia Road Conference. With more international activities expected to take place in Labuan Bajo, the reliability of the Flores power system is crucial.

Figure 1. Flores System Grid

This research utilizes the daily load profile data of the Flores power system for the year 2023, as shown in Figure 2. The data are categorized into two time zones for analysis, with 10:00 CIT (Central Indonesian Time) corresponding to a total load of 43.94 MW, representing the lowest system load, and 19:00 CIT with a total load of 84.77 MW, representing the system's peak load. The Flores system is already interconnected through distributed substations. Communication between these substations is facilitated via Optical Ground Wire (OPGW). This communication infrastructure is utilized by the Supervisory Control and Data Acquisition (SCADA) system for monitoring, operation, and coordination, as well as for system protection through a telecommunication channel. For the implementation of the Adaptive Load Shedding (ALS) system, the same communication channel used for system protection will also be utilized.

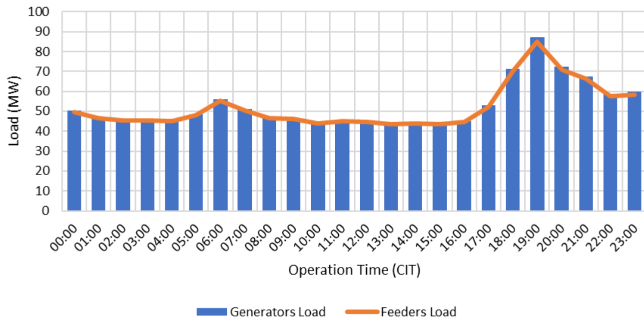

Figure 2. Flores System Load Profile 2023

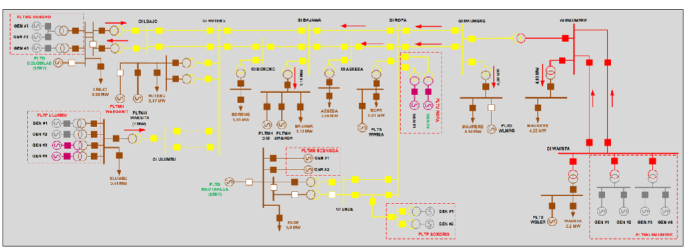

Figure 3. Flores System Overview

The existing UFLS target settings, as presented in Figure 4, have already been implemented in the Flores system based on previous simulations and studies that consider the inertia capability of the distributed generation units. The Under Frequency Load Shedding (UFLS) mechanism is divided into five distinct stages, each activated by a specific frequency threshold and implemented with a uniform delay time of 0.3 seconds to ensure a fast and coordinated response. If the system frequency continues to decline beyond these UFLS stages, the network transitions into Island Operation mode. This operation mode is designed to isolate and stabilize individual subsystems, preventing a complete system collapse. Two stages of Island Operation are defined to manage this condition. These settings have been implemented to consider the inertia characteristics of distributed generation within the system, aiming to optimize frequency response and ensure power supply continuity in critical scenarios. The existing defense scheme is designed to respond to loss of generation and load transfer events. Loss of generation refers to the sudden and unplanned disconnection of generation units from the power system, resulting in an immediate reduction of available generation capacity. This phenomenon can be triggered by various factors, including mechanical or electrical failures in generation equipment, the activation of protection systems in response to transient disturbances, disruptions in the primary energy supply (such as fuel shortages or variability in renewable energy sources), or external events like extreme weather conditions.

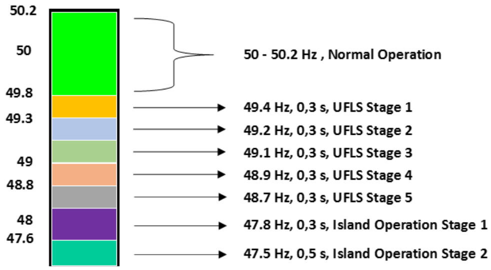

Figure 4. Flores Frequency Settings

The implementation of the existing defense scheme has been designed and adapted to align with the actual conditions of the power system, thereby enhancing system resilience and reliability in accordance with the operational requirements stipulated in the Grid Code issued by the Ministry of Energy and Mineral Resources (ESDM). Compliance with these provisions is reflected in the parameters and settings presented in Table 1.

Table 1. Operating frequency range limits [21].

Frequency Range	Operation Time Range
51,5 Hz $<f \leq$ 52,0 Hz	Operates for at least 15 minutes
51,0 Hz $<f \leq$ 51,5 Hz	Operates for at least 90 minutes
49,0 Hz $\leq f \leq$ 51,0 Hz	Operating continuously
47,5 Hz $<f<$ 49,0 Hz	Operates for at least 90 minutes
47,0 Hz $<f \leq$ 47,5 Hz	Operates for at least 6 seconds

[1] f : Grid Frequency.

3. Adaptive Load Shedding Mechanism

3.1 Load Shedding Scheme

Load shedding is a defense scheme used when there is an under-frequency cause of disturbance or loss of power generation or load transfer. There are two methods for implementing load shedding: manual load shedding, which operators or dispatchers execute, and automatic load shedding, which is executed by an Under Frequency Relay (UFR). The Under Frequency Load Shedding (UFLS) mechanism can respond rapidly to restore the system frequency to within permissible limits [22]-[23]. UFLS is typically used to release the load when the frequency exceeds its set value, along with the specified time delay. The System Frequency Response (SFR) model is a fundamental tool used to analyze the dynamic behavior of power systems in response to disturbances [24].

The procedure for simulating Adaptive Load Shedding (ALS) is based on the System Strength Index through several stages. First, system strength index data were collected, with the Flores Grid serving as the research object. The next step involved compiling UnderFrequency Load Shedding (UFLS) data obtained from the existing power system. Subsequently, a simulation model of the Flores power system was developed using DIgSILENT PowerFactory to accurately represent actual operating conditions. Following this, simulations were conducted, and performance data from the existing UFLS scheme were collected across nine disturbance scenarios at two different operational times.

The process continued with examining the operational principles of Adaptive Load Shedding, which was implemented using VBA Macro programming. As a basis for determining load-shedding targets, outgoing feeder load data were recorded at the two aforementioned time intervals. This data was then used to simulate the load sorting process based on a descending order method using VBA Macro. Additionally, simulations were conducted to exclude specific load-shedding targets, particularly for outgoing feeders in the Labuan Bajo Subsystem and other prioritized feeders, using VBA Macro configurations. Upon completing the configuration stages, simulations of the ALS scheme were executed, and performance data were gathered across the nine disturbance scenarios at the designated time intervals. Finally, a comparative analysis was performed to evaluate the performance between the existing UFLS scheme and the newly developed ALS scheme based on the System Strength Index.

3.2 System Strength Index

The System Strength Index (SSI) is a quantitative measure derived from historical data, reflecting the system's response to variations in conditions that affect loss generation, supply, or load transfers, particularly concerning frequency nadir decline. This index serves as an indicator of the operational reliability of the power system over a specific period. The SSI is formulated based on the existing operating conditions of the power system, which include the configuration and settings of the Under Frequency Load Shedding (UFLS) scheme implemented within the system. According to the 2023 Flores System Strength Index dataset, the relationship between load variations and frequency decline exhibits a linear trend, which can be expressed through a linear regression model, as shown in Equation (1).

$$y = 5,89y = 5,8965x + 2,7813 \tag{1}$$

In this Equation, y denotes the System Strength Index (SSI), which quantifies the system's ability to maintain operational stability in the face of disturbances. The variable x represents an independent system parameter that reflects disturbance-related characteristics, such as the ratio of lost active power to total generation capacity or lost load transfer in each subsystem. The regression coefficient of 5.8965 indicates that for every one-unit increase in x, the SSI increases by approximately 5.8965 units. Meanwhile, the constant term (intercept) of 2.7813 represents the baseline strength index when x=0, which may be interpreted as the minimum inherent system strength under no significant disturbance conditions. In the SSI formulation, the minimum threshold used is set at x = 0, as the focus of this study is on load shedding in response to generation loss or load transfer loss. This Equation was derived through linear regression analysis using historical or simulated disturbance data from the Flores power system. Integrating this model into the adaptive load-shedding mechanism allows the system to dynamically assess the appropriate load-shedding quantity based on real-time SSI values. This enables a more responsive and accurate defense strategy tailored to the system's condition during events such as generator trips or network disruptions.

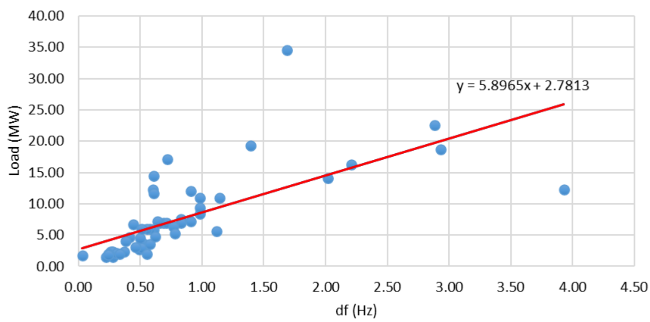

Figure 5. Flores System Strength Index 2023

The SSI approach was selected because it provides a correlated measure of the impact of generation loss or load transfer on the frequency nadir, thus serving as a predictive reference for estimating the potential impact of future contingencies. The Short Circuit Ratio (SCR) was not employed in this study, as it correlates short-circuit events with the response capacity of equipment or generators, which does not adequately capture the dynamic frequency response required for this analysis.

3.3 *Adaptive Load Shedding working scheme*

This study's Adaptive Load Shedding (ALS) mechanism calculates the load-shedding targets for each contingency case that occurs within the system. The ALS function is implemented using a research-based software tool [25] that employs the Microsoft Visual Basic for Applications (VBA) platform, as shown in Figure 6. VBA Macro is a programming language developed for Microsoft Office Excel, enabling the automation and dynamic execution of tasks within Excel.

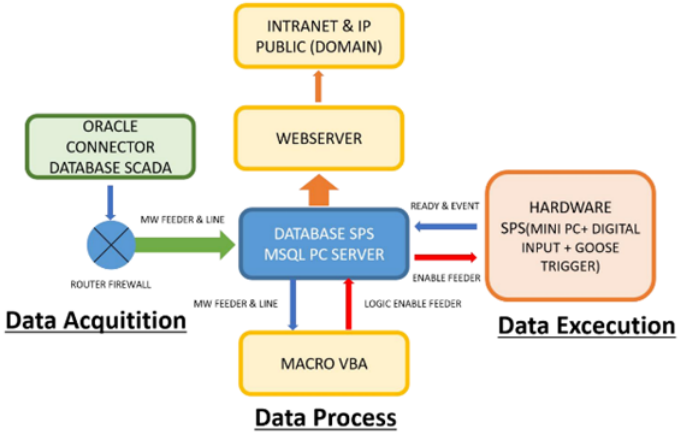

Figure 6. Macro VBA working scheme [25]

Real-time metering data, including feeder loads, generation output, and load transfer information sourced from Remote Terminal Units (RTUs) or Substation Automation Systems (SAS), are stored in a centralized MySQL database, which is then integrated with the VBA Macro using Open Database Connectivity (ODBC). The detection of contingency conditions and execution of load-shedding commands are facilitated through the IEC 61850 GOOSE (Generic Object Oriented Substation Event) messaging protocol, which allows for high-speed data exchange with execution times as fast as 100 milliseconds [12]. The data sorting method was also applied in the study [13], where Java–Bali load transfer data and load shedding target data were stored in a MySQL database. Subsequently, the load-shedding targets were sequentially sorted based on load magnitude and priority scale within the ADS optimization system and then utilized to generate arming signals for the required load-shedding targets according to the Java load transfer conditions. The study has not yet incorporated the calculation of the system strength index within the Bali subsystem, which is essential for improving the reliability of Energy Not Served (ENS) performance.

Figure 7 presents the detailed procedural flow of the server ALS algorithm, highlighting how it computes and selects appropriate load-shedding targets. The load-shedding execution is carried out using a Direct Transfer Trip (DTT) mechanism from the server to the Intelligent Electronic Device (IED) Input/Output (I/O) module. Furthermore, Figure 8 illustrates the overall architecture of the proposed Adaptive Load Shedding system, outlining the flow from the designated load-shedding targets to the server, which functions as the central processing unit. The server acquires metering data from substations or generators identified as part of the contingency case via the IEC 104 protocol. It then transmits an arming signal to initiate standby mode for load-shedding execution, following a decision-making process based on load prioritization and system requirements. Subsequently, the circuit breaker (CB) status from each IED I/O is exchanged using the GOOSE protocol according to the predefined logic under the supervision of the monitoring server. When a contingency condition is detected, the IED I/Os communicate with each other via a Direct Transfer Trip (DTT) to activate the load-shedding mechanism. The IED I/O shown in Figure 910 functions as the platform for implementing contingency logic based on circuit breaker (CB) status readings in accordance with the predetermined load-shedding targets. Upon initialization, the server transmits an arming signal via DTT to the IED I/O, instructing the device to enter a standby state. While in this state, the IED continuously monitors the system to determine whether the specified contingency case has occurred.

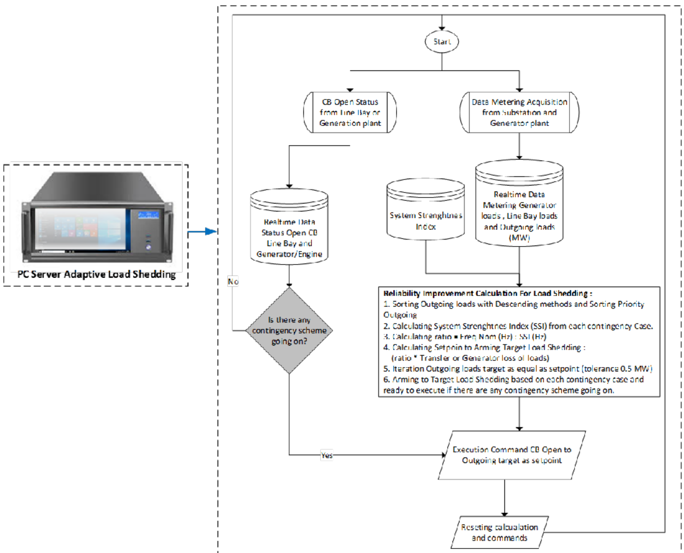

Figure 7. Adaptive Load Shedding Server Flowchart

4. Results and Discussions

Based on the Flores Grid configuration illustrated in Figure 3, this research evaluates nine disturbance study cases under lowest and peak load conditions. The study cases are defined as follows:

1. Trip of Diesel and Gas Power Plants (PLTMG) Maumere Units #2 and #3;
2. Trip of Steam Power Plant (PLTU) Ropa Unit #1;
3. Trip of Diesel and Gas Power Plants (PLTMG) Rangko Units #1 and #3;
4. Trip of Geothermal Power Plant (PLTP) Ulumbu Units #1, #3, and #4;
5. Trip of Diesel and Gas Power Plants (PLTMG) Rangko Units #1 and #3 together with Geothermal Power Plant (PLTP) Ulumbu Units #1, #3, and #4;
6. Trip of Steam Power Plant (PLTU) Ropa Unit #1 and Geothermal Power Plant (PLTP) Sokoria Units #1 and #2;
7. Trip of Overhead Lines (OHL) Ropa-Bajawa and Ropa-Aesesa, metering at the Ropa Substation side;
8. Trip of Overhead Line (OHL) Maumere-Wairita, metering at the Wairita Substation side; and

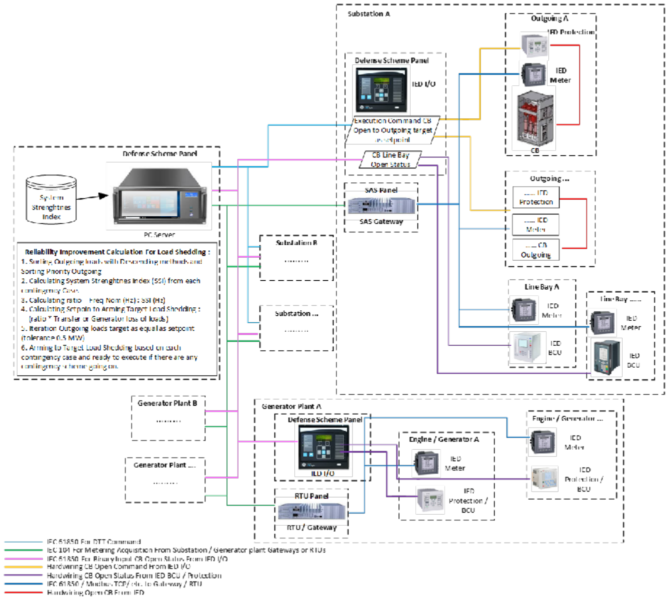

Figure 8. Adaptive Load Shedding Schematic System

9. Trip of Overhead Line (OHL) Maumere-Ropa, metering at the Maumere Substation side.

The generator trip study cases consider the system's operational reserve margin against N-1 contingencies, while the study cases involving the tripping of High Voltage Overhead Transmission Lines (OHL) are treated as N-2 contingencies. The causes of generator trips are attributed to transient disturbance responses that activate protection systems, as well as potential internal generator issues. In contrast, the tripping of two OHL lines results from protection system responses to faults, as the OHL network in this system remains radial in configuration. These study cases are designed to represent a diverse range of contingencies, including generation unit outages and transmission line failures, to comprehensively evaluate the proposed system's performance under varying operational conditions. Figure 9 shows study case 1 through 6 reflect various disturbance that did not lead to system islanding, with power transfer values ranging from 5.05 MW to 18.93 MW. Study case 7, 8, and 9 resulted in the separation of the system into two island regions, namely the western and eastern systems, with power transfer values ranging from 6.40 MW to 31.60 MW. The power transfer refers to the process of delivering electrical power from one part of the power system to another, either between generation units and loads or across interconnected areas of the system. The magnitude of power transfer typically represents the amount of active power (measured in MW) transmitted through specific transmission lines or interconnections. In study case 7, the system will divided into two electrical islands. The western island includes the Labuan Bajo, Ruteng, Borong, Bajawa, and Aesesa subsystems, while the eastern island comprises the Ropa, Ende, Maumere, and Wairita subsystems. In study case 8, the system will divided into two islands where the western island consists of the Labuan Bajo, Ruteng, Borong, Bajawa, Aesesa, Ropa, Ende, and Maumere subsystems, and the eastern island is limited to the Wairita subsystem. In study case 9, the system will be divided into two islands. The western island contains the Labuan Bajo, Ruteng, Borong, Bajawa, Aesesa, Ropa, and Ende subsystems, while the eastern island consists of the Maumere and Wairita subsystems.

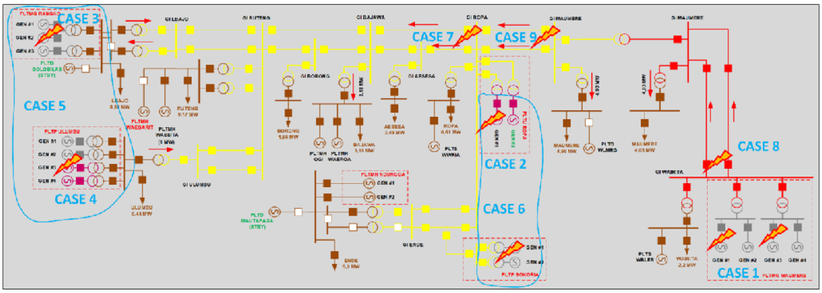

Figure 9. SLD Interpretation of the Simulation Study Case

In study case 7, the metering readings are located at the Ropa substation, and the CB status acquisitions are at the Ropa, Bajawa, and Aesesa Substation. As a result, the load flow calculated by the Western system during islanding reflects the load transferred towards the Bajawa and Aesesa substations. However, if the direction of load transfer is towards the Ropa substation, the Automatic Load Shedding (ALS) triggered by the circuit breaker (CB) at Ropa, Bajawa, and Aesesa Substation does not account for the ALS scheme. This is because the ALS load magnitude falls under the operational domain of metering readings on the Aesesa and Bajawa substations, which is not included in this study case.

In study case 8, the metering readings are located at the Wairita substation, and the CB status acquisitions are at both the Wairita and Maumere Substations. Consequently, the load flow calculated by the Western system during islanding reflects the load being transferred towards the Maumere substation. However, suppose the direction of load transfer is towards the Wairita substation. In that case, the ALS triggered by the CB at GI Wairita and Maumere does not account for the ALS scheme since the corresponding ALS load falls under the operational scope of metering readings on the Maumere Substation, which is not considered in this study case.

In study case 9, the metering readings are located on the Maumere substation. Therefore, the load flow calculated by the Western system during islanding represents the load transferred towards the Ropa substation. However, suppose the direction of load transfer is towards the Maumere substation. In that case, the ALS triggered by the CB at Maumere and Ropa substation does not account for the ALS scheme, as the relevant ALS load belongs to the operational domain of metering readings on the Ropa substation, which is not included in this study case. The effectiveness of the adaptive load-shedding strategy has been demonstrated in post-islanding system configurations, significantly reducing ENS in both regions of the power system.

4.1 Study case simulation at lowest load

The results of the simulation are illustrated in Figure 10. In cases 2, 4, 5, and 6, the ENS under the ALS scheme is observed to be higher than that of the existing UFLS scheme. This is primarily due to the ALS scheme's consideration of real time load transfer or supply conditions, which are adjusted based on the ratio between the System Stability Index (SSI) and the nominal frequency. In study case 2, the ENS under the ALS scheme is 1.51 MWh higher than that of the UFLS scheme. However, based on the system frequency response shown in Figure 12, the ALS scheme demonstrates an improved frequency decline profile, with the lowest frequency reaching 49.74 Hz, compared to 49.27 Hz in the existing UFLS scheme.

Similarly, in study case 4, the simulation results align with those of study case 2 due to comparable generation supply loads at lowest load, approximately 5.95 MW. As shown in Figure 14, study case 4 also exhibits a less steep frequency decline under the ALS scheme, with a minimum frequency of 49.83 Hz, whereas the UFLS scheme yields a minimum of 49.31 Hz. In study case 5, which represents the condition with the highest generation supply load of 16.99 MW, the ENS under the ALS scheme is 0.14 MWh higher than the existing UFLS scheme. Nevertheless, as shown in Figure 15, the ALS scheme achieves a notable improvement in frequency response, with a minimum of 49.18 Hz, compared to 48.41 Hz in the UFLS scheme. For study case 6, the ALS scheme results in an ENS of 0.34 MWh higher than that of the UFLS scheme. However, as illustrated in Figure 16, the ALS scheme still delivers a smoother frequency drop, with a minimum frequency of 49.58 Hz, whereas the UFLS scheme drops to 49.03 Hz.

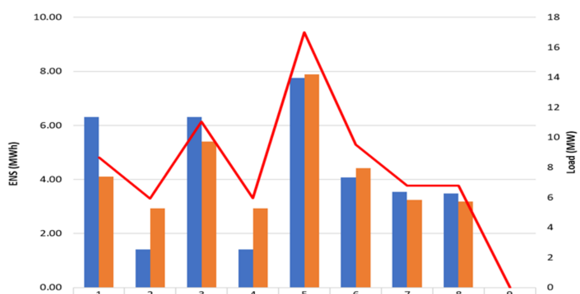

	1	2	3	4	5	6	7	8	9
UFLS Response	6.31	1.42	6.31	1.42	7.75	4.08	3.54	3.48	0.00
ALS Response	4.11	2.93	5.41	2.93	7.89	4.42	3.24	3.18	0.00
Load Transfer / Supply	8.65	5.94	11.04	5.95	16.99	9.51	6.8	6.8	0

Figure 10. ENS results in each study case based on UFLS and ALS at lowest load.

Although the ALS scheme in study cases 2, 4, 5, and 6 resulted in a higher ENS compared to the existing UFLS scheme, the overall performance of the ALS scheme across all nine study cases yielded a total ENS of 34.08 MWh. In contrast, the total ENS under the existing UFLS scheme was 34.29 MWh. This indicates a reliability improvement of 0.61% in favor of the ALS scheme. The most significant ENS reliability improvement using the ALS scheme was observed in study case 1, with a reduction of 2.2 MWh, equivalent to an enhancement of 34.94% compared to the existing UFLS scheme. In study case 9, the power flow is directed toward the Maumere

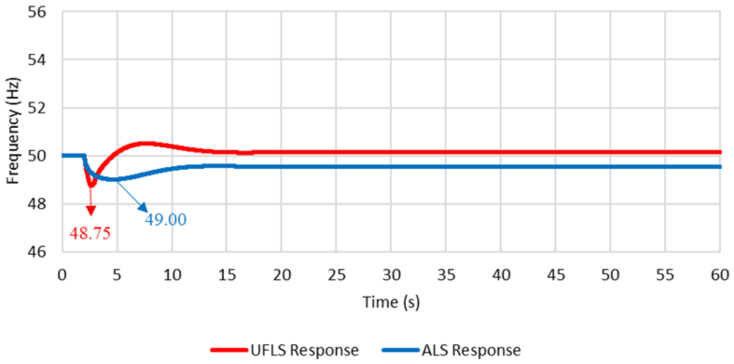

Figure 11. Frequency response on study case 1 at lowest load.

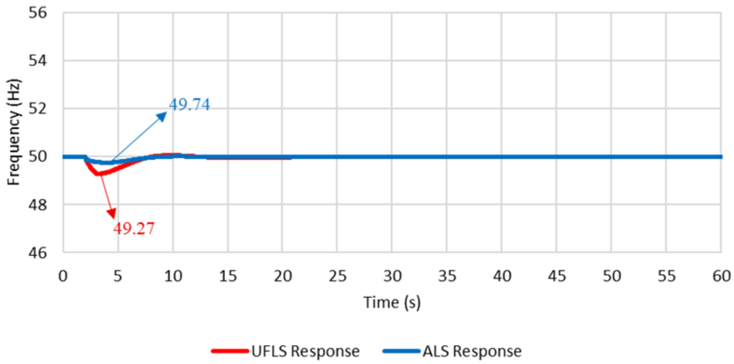

Figure 12. Frequency response on study case 2 at lowest load.

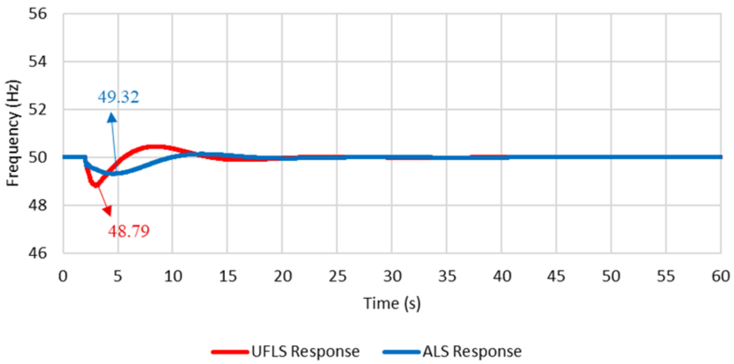

Figure 13. Frequency response on study case 3 at lowest load.

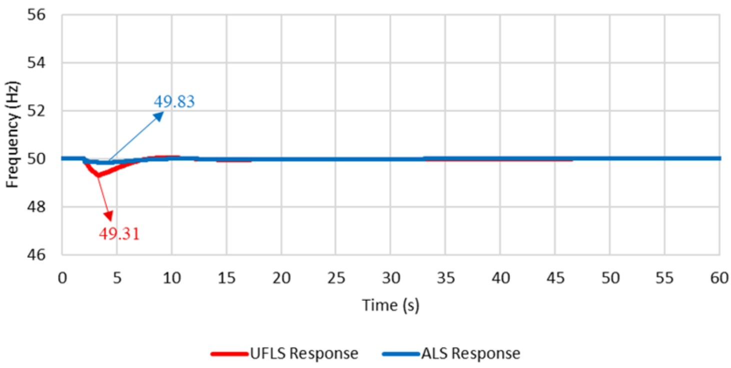

Figure 14. Frequency response on study case 4 at lowest load.

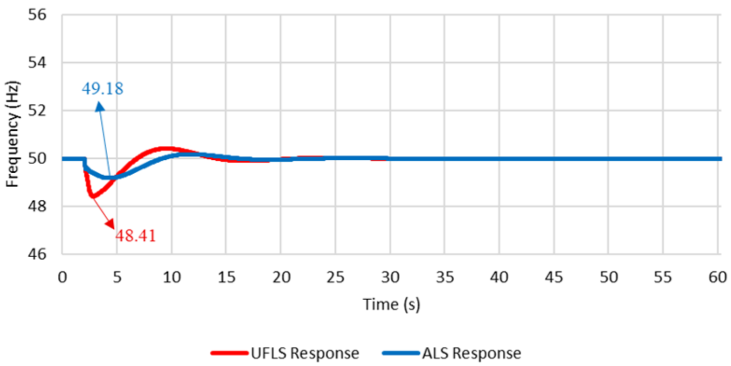

Figure 15. Frequency response on study case 5 at lowest load.

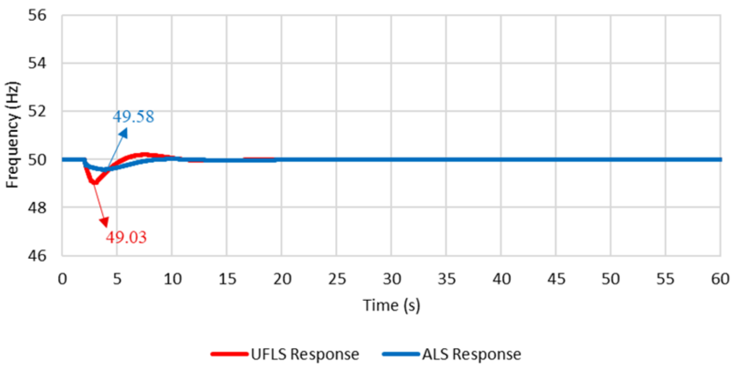

Figure 16. Frequency response on study case 6 at lowest load.

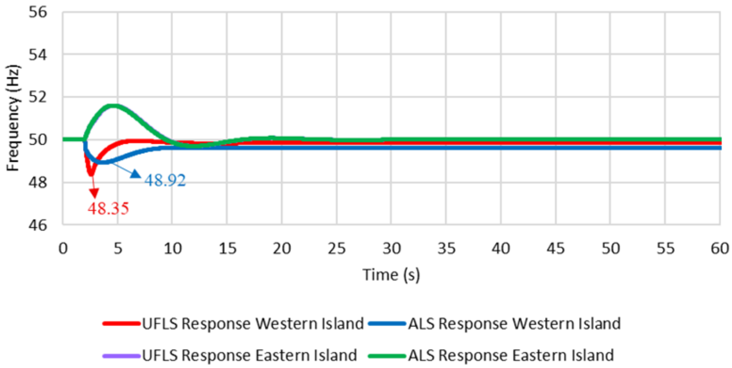

Figure 17. Frequency response on study case 7 at lowest load.

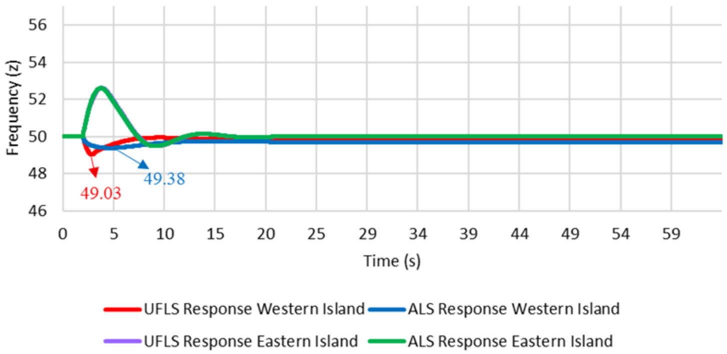

Figure 18. Frequency response on study case 8 at lowest load.

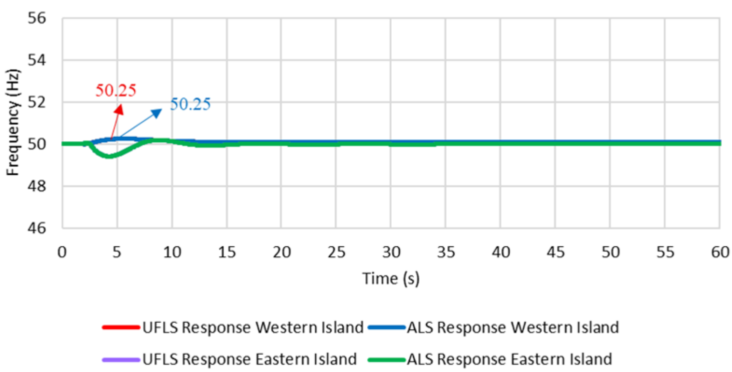

Figure 19. Frequency response on study case 9 at lowest load.

Substation, resulting in a negative metering load reading on the Ropa–Maumere overhead line (OHL) at the Maumere Substation. Consequently, during the contingency event in study case 9, the defense scheme did not trigger the activation of the Adaptive Load Shedding (ALS) mechanism.

This improvement in ALS reliability also positively impacts the steady state frequency condition of the system following disturbances. Nonetheless, based on Figures 11–19, the frequency steady state responses observed across study cases 1 to 9 remain within the permissible operational limits as defined by the prevailing grid code regulations, and ALS can enhance the damping of frequency nadirs.

4.2 Study case simulation at peak load

At peak load,simulations were conducted using the same nine study cases as in the previous scenario. The results of ENS for both the ALS and the existing UFLS) schemes are presented in Figure 20. In several cases, specifically study cases 2, 3, 4, and 6, the ALS scheme yielded higher ENS values than the existing UFLS scheme. In the remaining study cases, the ALS scheme demonstrated superior performance by producing lower ENS values.

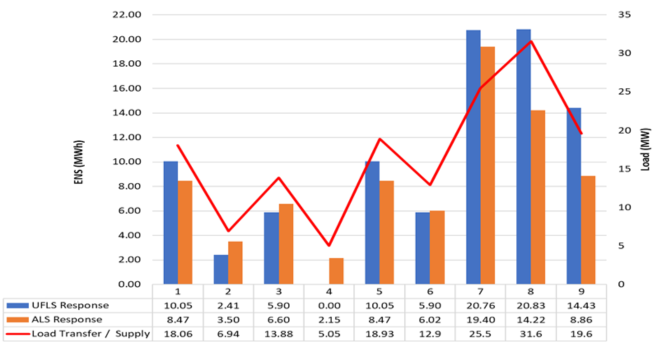

Figure 20. ENS results in each study case based on UFLS and ALS at peak load

In study case 2, the system experienced a generation loss of 6.94 MW. The ALS scheme resulted in an ENS value of 1.09 MWh, which is greater than the existing UFLS scheme. Nevertheless, as illustrated in Figure 22, the ALS scheme improved the rate of frequency decline, with the lowest frequency recorded at 49.83 Hz, compared to 49.32 Hz under the existing UFLS scheme.In study case 3, a generation loss of 13.88 MW occurred, and the ALS scheme produced an ENS 0.7 MWh higher than that of the UFLS scheme. However, as shown in Figure 23, the ALS scheme effectively mitigated the frequency drop, with a minimum frequency of 49.81 Hz, whereas the existing UFLS scheme reached a lower value of 49.07 Hz. In study case 4, the system lost 5.05 MW of generation capacity. The ALS scheme resulted in an ENS value of 2.15 MWh higher than that of the UFLS scheme. Nevertheless, Figure 24 shows that the ALS scheme significantly improved the frequency response, achieving a minimum frequency of 49.96 Hz, compared to 49.63 Hz for the existing UFLS. Notably, in this case, the UFLS scheme did not operate because the remaining generators were sufficient to maintain system stability within acceptable frequency limits.

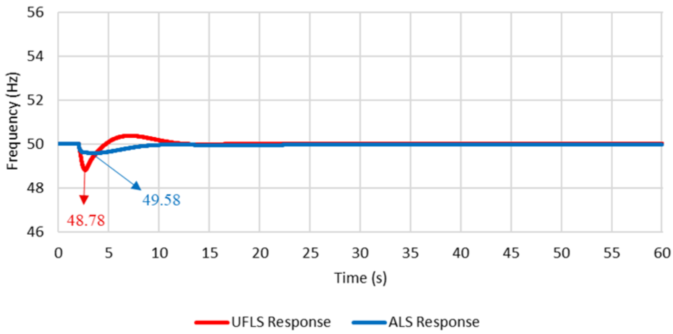

Figure 21. Frequency response on study case 1 at peak load.

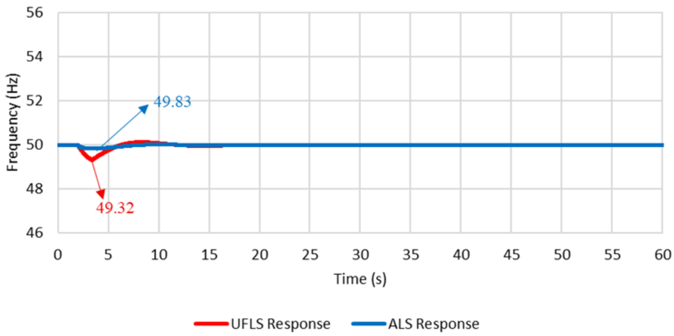

Figure 22. Frequency response on study case 2 at peak load.

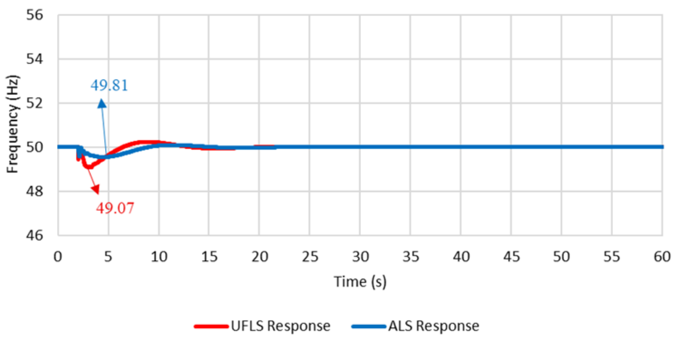

Figure 23. Frequency response on study case 3 at peak load.

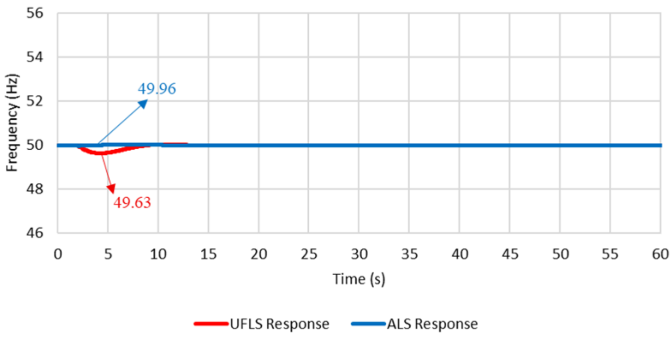

Figure 24. Frequency response on study case 4 at peak load.

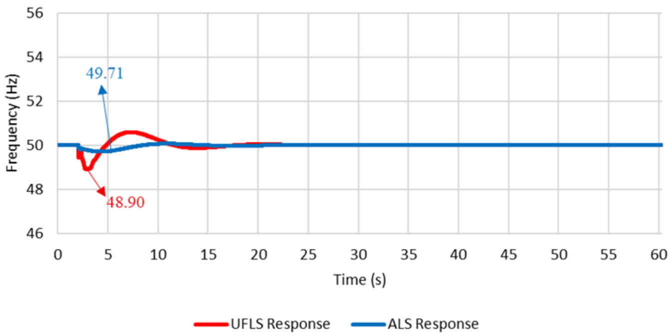

Figure 25. Frequency response on study case 5 at peak load.

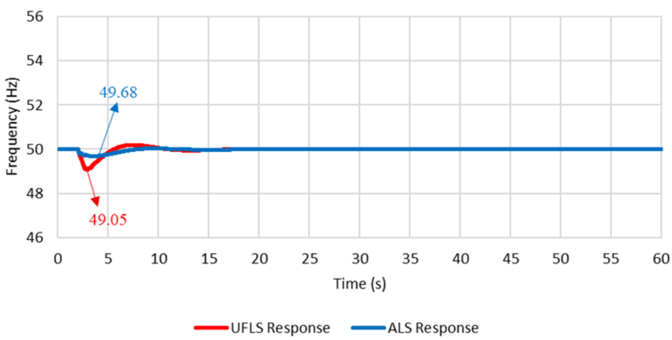

Figure 26. Frequency response on study case 6 at peak load.

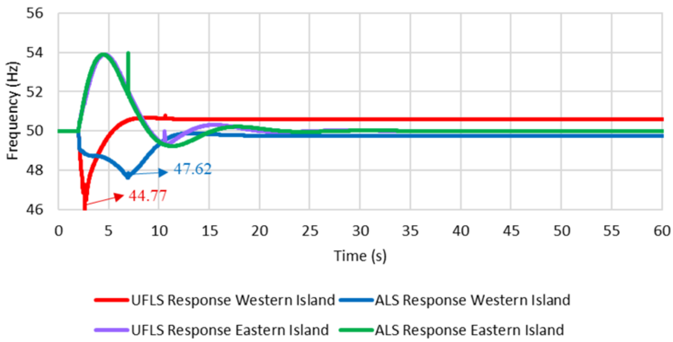

Figure 27. Frequency response on study case 7 at peak load.

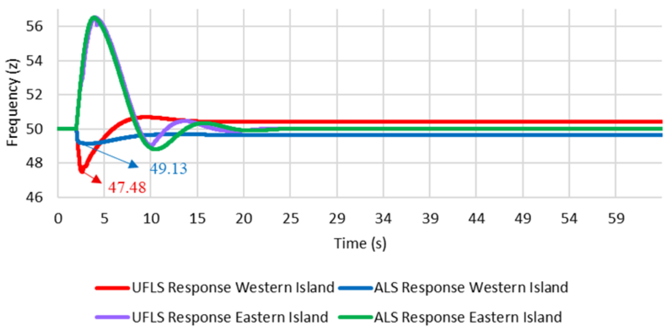

Figure 28. Frequency response on study case 8 at peak load.

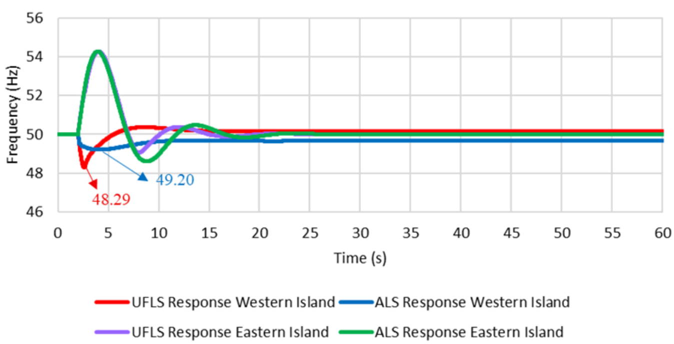

Figure 29. Frequency response on study case 9 at peak load.

In study case 6, the system experienced a generation loss of 12.9 MW, with the ALS scheme yielding an ENS 0.12 MWh higher than the existing UFLS scheme. Nonetheless, Figure 26 demonstrates that the ALS scheme improved the frequency decline profile, recording a minimum frequency of 49.68 Hz, compared to 49.05 Hz for the existing UFLS. These findings suggest that although ALS may produce higher ENS in certain scenarios, its ability to mitigate the severity of frequency deviations indicates a beneficial impact on the system's dynamic frequency stability.

Although the ALS scheme produced higher ENS values in study cases 2, 3, 4, and 6 compared to the existing UFLS scheme, the overall performance of ALS across all nine study cases yielded a total ENS of 77.66 MWh. In contrast, the existing UFLS scheme resulted in a total ENS of 90.31 MWh. This reflects a 14.01% reliability improvement in favor of the ALS scheme. The most significant reliability gain achieved by the ALS scheme occurred in study case 8, where the ENS was reduced by 6.60 MWh, corresponding to a 31.72% improvement relative to the UFLS scheme. This enhancement in ENS reliability under the ALS approach also positively influenced the system's frequency steady state conditions following a disturbance. Nevertheless, the frequency steady state response across all nine study cases remained within the acceptable limits of the prevailing grid code requirements.

5. Conclusions

The simulation study conducted on nine disturbance study cases and two system load conditions scenarios, lowest load (at 10:00 CIT) and peak load (at 19:00 CIT). This research demonstrates that the proposed Adaptive Load Shedding (ALS) scheme provides a significant improvement in power system reliability performance compared to the existing Under Frequency Load Shedding (UFLS) scheme. The total Energy Not Served (ENS) reduction achieved by the ALS scheme was recorded at 0.61% during the lowest load condition, and a reliability improvement of 14.01% was achieved during the peak load condition. The average improvement achieved by the ALS scheme is 7.31%, consistently demonstrating superior dynamic performance in mitigating the rate of frequency decline. It presents a promising solution for enhancing contingency management in the Flores power system, particularly in isolated systems or networks with weak interconnections.

The transition from the existing UFLS defense scheme to an ALS-based scheme requires several system preparations and investments. These include establishing telecommunication links between substations and generating units, utilizing Optical Ground Wire (OPGW), acquiring metering data from each substation and generator through Gateways or Remote Terminal Units (RTUs) supported by IEC 60870-5-104 protocol to enable data management by the ALS server and ensuring the readiness of Intelligent Electronic Devices (IEDs) at substations and generating units, which must support IEC 61850 protocol to allow the arming scheme and Direct Transfer Trip (DTT) functions to operate effectively within the ALS system.

References

[1] M. A. Kabir, A. H. Chowdhury, and N. Al Masood. "A Dynamic-Adaptive Load Shedding Methodology to Improve Frequency Resilience of Power Systems". In: *International Journal of Electrical Power & Energy Systems* 122 (2020). DOI: 10.1016/j.ijepes.2020.106169.

[2] S. F. Abrar and N. Al Masood. "An Adaptive Load-Shedding Method for Renewable Integrated Power Systems". In: *Proceedings of the 2023 International Conference on Power, Instrumentation, Control and Computing (PICC)*. IEEE, 2023.

[3] A. Hadavi, M. T. Hagh, and S. G. Zadeh. “Critical Inertia Thresholds for Frequency Stability in Renewable Energy-Integrated Power Systems”. In: *International Journal of Electrical Power & Energy Systems* 169 (2025). DOI: 10.1016/j.ijepes.2025.110733.

[4] C. Wang et al. “A Two-Stage Underfrequency Load Shedding Strategy for Microgrid Groups Considering Risk Avoidance”. In: *Applied Energy* 367 (2024). DOI: 10.1016/j.apenergy.2024.123343.

[5] M. Marzband et al. “Adaptive Load Shedding Scheme for Frequency Stability Enhancement in Microgrids”. In: *Electrical Power and Energy Systems Research* 140 (2016), pp. 78–86. DOI: 10.1016/j.epsr.2016.06.037.

[6] L. Sigrist, L. Rouco, and F. M. Echavarren. “A Review of the State of the Art of UFLS Schemes for Isolated Power Systems”. In: *International Journal of Electrical Power & Energy Systems* 99 (2018), pp. 525–539.

[7] G. M. Njoka, L. Mogaka, and A. Wangai. “Impact of Variable Renewable Energy Sources on the Power System Frequency Stability and System Inertia”. In: *Energy Reports* 12 (2024), pp. 4983–4997. DOI: 10.1016/j.egyr.2024.10.057.

[8] T. Shekari, F. Aminifar, and M. Sanaye-Pasand. “An Analytical Adaptive Load Shedding Scheme against Severe Combinational Disturbances”. In: *IEEE Transactions on Power Systems* 31 (2016), pp. 4135–4143. DOI: 10.1109/TPWRS.2015.2503563.

[9] J. Tang et al. “Adaptive Load Shedding Based on Combined Frequency and Voltage Stability Assessment Using Synchrophasor Measurements”. In: *IEEE Transactions on Power Systems* 28 (2013), pp. 2035–2047. DOI: 10.1109/TPWRS.2013.2241794.

[10] W. E. P. S. Ediriweera and N. W. A. Lidula. “Adaptive Load Shedding Technique for Energy Management in Networked Microgrids”. In: *Proceedings of the 2023 IEEE 17th International Conference on Industrial and Information Systems (ICIIS)*. IEEE, 2023, pp. 465–470.

[11] T. Baškarad et al. “Dynamically Adaptive Method for under Frequency Load Shedding Protection Scheme Reconfiguration”. In: *Electrical Power Systems Research* 207 (2022). DOI: 10.1016/j.epsr.2022.107823.

[12] P. D. Putra and M. P. Marbun. “Adaptive Defense Scheme Implementation in Muarakarang Subsystem to Prevent Island Operation Failure”. In: *Proceedings of the 11th EECCIS*. IEEE, 2022, pp. 88–93.

[13] A. Sofwan et al. “Post Operational Optimization of Adaptive Overload Shedding Protection in the Bali Island Subsystem Using the ADS Simulation”. In: *International Journal of Advanced Multidisciplinary* 2 (2024). DOI: 10.38035/ijam.v2i4.

[14] H. Haes Alhelou et al. “An Overview of UFLS in Conventional, Modern, and Future Smart Power Systems: Challenges and Opportunities”. In: *Electrical Power Systems Research* 179 (2020).

[15] J. Yang et al. “Response-Driven Adaptive under Frequency Load Shedding Scheme Based on Energy Model”. In: *Electrical Power Systems Research* 238 (2025). DOI: 10.1016/j.epsr.2024.111150.

[16] M. Rajabdorri et al. “Data-Driven Estimation of the Amount of under Frequency Load Shedding in Small Power Systems”. In: *Engineering Applications of Artificial Intelligence* 139 (2025). DOI: 10.1016/j.engappai.2024.109617.

[17] A. Ketabi and M. Hajiakbari Fini. “Adaptive Underfrequency Load Shedding Using Particle Swarm Optimization Algorithm”. In: *Journal of Applied Research and Technology* 15 (2017), pp. 54–60. DOI: 10.1016/j.jart.2016.12.003.

[18] M. Muftić Dedović et al. “Enhancing Power System Stability with Adaptive under Frequency Load Shedding Using Synchrophasor Measurements and Empirical Mode Decomposition”. In: *International Journal of Electrical Power & Energy Systems* 160 (2024). DOI: 10.1016/j.ijepes.2024.110133.

[19] W. Jinhua and B. Yanyan. “An Optimal Adaptive under Frequency Load Shedding Using Artificial Neural Networks”. In: *Proceedings of the 2022 IEEE International Conference on Electrical Engineering, Big Data and Algorithms (EEBDA)*. IEEE, 2022, pp. 249–253.

[20] S. S. Silva and T. M. L. Assis. “Adaptive Underfrequency Load Shedding in Systems with Renewable Energy Sources and Storage Capability”. In: *Electrical Power Systems Research* 189 (2020). DOI: 10.1016/j.epsr.2020.106747.

[21] Kementerian Energi dan Sumber Daya Mineral. *Peraturan Menteri Energi dan Sumber Daya Mineral Nomor 20 Tahun 2020 tentang Aturan Jaringan Sistem Tenaga Listrik (Grid Code)*. Jakarta, Indonesia, 2020.

[22] D. R. Alwaini and H. S. Dini. "Design of Defense Scheme Based on Adaptive under Frequency Load Shedding (AUFLS) at Lombok Island Grid System". In: *Proceedings of the 2021 3rd International Conference on High Voltage Engineering and Power Systems (ICHVEPS)*. IEEE, 2021, pp. 117–121.

[23] PT PLN (Persero). *Standard of PT PLN (Persero) S5.005-2022 – Pedoman Perencanaan dan Implementasi Sistem Defense Scheme*. 2022.

[24] H. Bentarzi. *PMU Based Centralized Adaptive Load Shedding Scheme in Power System*.

[25] A. B. Zakaria, R. Nuringtyas, and A. Hardoyo. "Special Protection System with Macro VBA-based Descending Method at PT PLN (Persero) South and Central Kalimantan". In: *Proceedings of the International Conference on Technologies and Policies in Electric Power & Energy*. 2019, pp. 1–4.